



HAL
open science

Shrinking and Splitting of drainage basins in orogenic landscapes from the migration of the main drainage divide

Stéphane Bonnet

► **To cite this version:**

Stéphane Bonnet. Shrinking and Splitting of drainage basins in orogenic landscapes from the migration of the main drainage divide. *Nature Geoscience*, 2009, 2, pp.766 - 771. 10.1038/ngeo666 . insu-00429309

HAL Id: insu-00429309

<https://insu.hal.science/insu-00429309>

Submitted on 3 Nov 2009

HAL is a multi-disciplinary open access archive for the deposit and dissemination of scientific research documents, whether they are published or not. The documents may come from teaching and research institutions in France or abroad, or from public or private research centers.

L'archive ouverte pluridisciplinaire **HAL**, est destinée au dépôt et à la diffusion de documents scientifiques de niveau recherche, publiés ou non, émanant des établissements d'enseignement et de recherche français ou étrangers, des laboratoires publics ou privés.

1 Shrinking and Splitting of drainage basins in orogenic 2 landscapes from the migration of the main drainage divide

3 STEPHANE BONNET ^{1,2}

4 ¹Géosciences Rennes, Université de Rennes 1, Campus de Beaulieu, 35042 Rennes Cedex, France

5 ²CNRS/INSU, UMR 6118, Campus de Beaulieu, 35042 Rennes Cedex, France

6 e-mail: stephane.bonnet@univ-rennes1.fr

7 Phone +33 2 23 23 56 90

8 Fax +33 2 23 23 67 80

9

10 **Climate, and in particular the spatial pattern of precipitation, is thought to affect the**
11 **topographic and tectonic evolution of mountain belts through erosion¹⁻⁵. Numerical model**
12 **simulations of landscape erosion controlled by horizontal tectonic motion⁶ or orographic**
13 **precipitation^{7,8} result in the asymmetric topography that characterizes most natural mountain**
14 **belts⁶, and in a continuous migration of the main drainage divide. The effects of such a**
15 **migration have, however, been challenging to observe in natural settings⁶. Here I document**
16 **the effects of a lateral precipitation gradient on a landscape undergoing constant uplift in a**
17 **laboratory modelling experiment. In the experiment, the drainage divide migrates towards the**
18 **drier, leeward side of the mountain range, causing the drainage basins on the leeward side to**
19 **shrink and split into smaller basins. This mechanism results in a progressively increasing**
20 **number of drainage basins on the leeward side of the mountain range as the divide migrates,**
21 **such that the expected relationship between the spacing of drainage basins and the location of**
22 **the main drainage divide⁹ is maintained. I propose that this mechanism could clarify the**
23 **drainage divide migration and topographic asymmetry found in active orogenic mountain**
24 **ranges, as exemplified by the Aconquija Range of Argentina¹⁰.**

25

26 In separating the water flux coming from precipitation between the drainage basins located
27 over the two opposite flanks of topography, the main drainage divide is an important physiographic
28 element of orogen topography. When associated with an orographic effect, drainage divide
29 delineates domains where differences in precipitation and hydrologic regimes may directly influence
30 erosional processes that shape topography and thus, landscape forms^{7,8}, erosion rates¹¹ and, over a
31 geological time-scale, the rates and patterns of exhumation of metamorphic rocks⁴ and internal
32 strain³ within the orogens. The continuous migration of the drainage divide in orogens, as observed
33 in the numerical modelling of surface processes when erosion is forced by tectonic advection⁶ or
34 orographic precipitations^{7,8}, is hardly demonstrable in natural settings. Only the observation that
35 natural orogens usually exhibit asymmetric topography⁶ supports numerical results. In natural
36 settings, divide dynamics have only been inferred in local and timely-discontinuous shifts in their
37 location consecutive to river capture events¹². They have also occasionally been inferred from
38 changes in sediment content at the drainage basin outlets¹³. This emphasizes the need to find criteria
39 that can be used to better investigate divide migration in orogens.

40 The experimental modelling of erosion is a powerful tool to investigate landscape dynamics.
 41 It indicates that landscapes may be more dynamic than the numerical models suggest¹⁴, e.g. when
 42 considering the evolution of ridge crests, and it has already been used to demonstrate that some
 43 landscape features, such as long narrow perched drainages, form in areas of actively migrating
 44 divides¹⁵. Figure 1 shows an example of divide migration in the laboratory modelling of landscape
 45 dynamics^{16,17} forced by uniform uplifting of the eroded material but with a precipitation gradient (see
 46 the Methods section). In this experiment, the precipitation gradient was applied after a first phase of
 47 uniform precipitation and the attainment of a steady state between erosion and uplift^{16,17} (Fig. 1).
 48 During this initial phase, the topography is symmetric overall (Fig. 1a, Fig. 1c), and the elevation of
 49 the divide remains constant with time (Fig. 1a, Fig. 1b). Application of the precipitation gradient
 50 induces migration of the drainage divide toward the drier side of the landscape and development of
 51 an asymmetric topography (Fig. 1), as also observed numerically^{7,8}. The divide is simultaneously
 52 uplifted (Fig. 1b) such that the mean topographic slope of the wetter side of the landscape remains
 53 constant during its elongation (Fig. 1a). At no time is the establishment of a new steady-state
 54 observed in this experiment (Fig. 1b), nor is the divide position pinned (Fig. 1c). The progressive
 55 shortening of the drier side of the landscape consecutive to divide migration results in an increase in
 56 the roughness of the surface and in a very unstable landscape (Fig. 2). This leads to an original
 57 mechanism that splits the drainage networks: each initial drainage network splits into two individual
 58 networks that become progressively separated by the growth of a new hillcrest (Figure 2). Through
 59 this mechanism, the numbers of drainage basins extending to the main divide increases during divide
 60 migration.

61 Given the pattern of rainfall and once the precipitation gradient is applied, the migration of
 62 the drainage divide induces a continuous decrease in the mean runoff within the drainage basins
 63 located on the drier side of the landscape (Fig. 3b). There, the area of the drainage basins decreases
 64 because of the combination of two processes: a continuous size reduction (a direct consequence of
 65 the divide migration), and an abrupt size reduction consecutive to the split of the drainage network
 66 and the individuation of two drainage basins from a previous single one. Overall, the decrease of the
 67 drainage basins' size correlates with a steepening of their channels (Fig. 3c). The detailed analysis of
 68 the experimental drainage basins' response to the rainfall gradient documents a two-step evolution
 69 of the channels, before and after splitting occurred (Fig. 3). In a first phase, from the establishment of
 70 the precipitation gradient up to the splitting, an erosion wave propagates upward within the former
 71 steady-state channels (Fig. 3c). It generates the upstream migration of a knickpoint, defined as an
 72 abrupt change in the channel gradient, which separates an upstream segment passively uplifted from
 73 a downstream segment steepened to a new steady-state gradient (Fig. 3c). This mechanism has
 74 already been described analytically^{18,19} and experimentally¹⁶. After the erosion wave has swept the
 75 entire channels, channel steepening drives a temporary steady-state between uplift and erosion (Fig.
 76 3 c,d). This temporary steady-state only concerns channels and not the whole landscape (Fig. 1), as
 77 hillcrests are passively uplifted at the same time (Fig. 3d). In a second phase, after the split of
 78 drainage networks, a profound disruption of the temporary steady-state of the channels occurs,
 79 preventing the establishment of new steady-state conditions. From splitting onward, the channels
 80 continuously steepen as they shorten because of divide migration (Fig. 3c). Figure 3d shows the
 81 elevation history of three geographically-fixed spatial points of the model, illustrating how complex
 82 elevation histories can be during this sequence of landscape changes. Specifically, it illustrates how

83 some parts of the floodplains are uplifted and transformed into a divide separating the two newly-
84 formed drainage basins after splitting has occurred.

85 As for natural channels²⁰, the hydraulic properties, width, depth, cross-sectional area, mean
86 flow velocity, hydraulic radius and wet perimeter all increase with water discharge in the
87 laboratory²¹. By continually reducing the discharge within drainage basins, divide migration
88 consequently drives a narrowing of the channels so that erosion is progressively localized within the
89 floodplains during divide migration, resulting in their abandoned parts being uplifted (Fig. 3d).
90 Channels have also been shown to narrow as they steepen, theoretically²² and in the field²³, so that
91 narrowing may also be driven by the steepening of the channels described here (Fig. 3c). Even if
92 channels cannot be observed directly during experiments because of opacity during rainfall, a careful
93 examination at the time-step evolution of the experimental landscape (Fig. 2) shows that the location
94 of the newly-formed trunk channels after splitting is intimately linked to the former geometry of the
95 upstream tributaries of the channel network. As illustrated in Figure 4, the network splitting
96 mechanism most likely occurs at the tributaries' junction and lies in the combination of channel
97 narrowing associated with ongoing uplift and reduced erosion rates in the interfluvies area (Fig 3d).
98 This enables flows coming from the tributaries to disconnect in place of a former single channel.

99
100 The mechanism of network splitting proposed here led to transient dynamics that are
101 exemplified by the Sierra Aconquija range in the Sierras Pampeanas province of NW Argentina¹⁰ (Fig.
102 5). The Aconquija is an uplifted basement range, bounded by active high-angle reverse faults on one
103 or both sides against Neogene sedimentary basins^{10,24-25} (Fig. 5). Thermochronological data¹⁰
104 indicates the start of the rapid exhumation of the range ~6 Ma ago and a total rock uplift of at least
105 6.4-11.1 km over the last 6 Myr. It presently forms a prominent landscape above its adjacent
106 foreland plains, reaching elevations > 5 km. Because of its location on the eastern front of the Andes,
107 representing a major topographic barrier to the moisture flux coming from the Atlantic Ocean²⁶, the
108 Sierra Aconquija is an orographic barrier: its eastern flank receives much more precipitation (> 2 m
109 yr⁻¹) than its western one^{10,25-26} (Fig. 5), where an arid climate prevails. To the west of the Aconquija,
110 climate proxies indicate that aridification initiated 3 Myr ago²⁷. It is interpreted as reflecting the
111 onset of the orographic barrier via a surface uplift of the Aconquija²⁷, which occurred when the
112 topography reached elevations of 2-2.5 km in the Andes¹⁰. Compared to modern maximum
113 elevations of the range, this suggests that the divide of the Aconquija has been uplifted (surface
114 uplift) by 3-3.5 km during the last 3 Myr¹⁰. The Aconquija presently shows a jagged topography
115 characterized by deeply-incised, regularly-spaced, transverse rivers. Overall, its topography is
116 asymmetric and its drainage divide shows an offset position toward the drier side of the range (Fig.
117 5), with a fractional divide position⁶ of 0.6-0.7. The drainage networks on the drier leeward flank of
118 the range show multiple examples of unusual landscape configurations (Fig. 5c), indicating that the
119 split of drainage networks likely occurred following the mechanism described experimentally (Fig. 4).
120 It implies the migration of the main divide of the Aconquija toward the drier flank of the range and
121 the progressive development of its topographic asymmetry. The asymmetric development of
122 topography would not exist in the absence of asymmetry of at least one forcing parameter⁶: rock
123 erodability, tectonic forcing or climatic conditions. Differences in erodability are not likely to be the
124 cause of the asymmetry because variations in topography do not coincide with lithologic ones.
125 Horizontal tectonic motions are likely negligible in the Aconquija case because of the high-angle of

126 the bounding faults^{10,24} and because the range is bounded by opposite reverse faults on both sides in
 127 the area considered (Fig. 5). The development of the topographic asymmetry of the Aconquija is
 128 most likely the direct result of climate, through the establishment of the orographic rainfall gradient,
 129 following a mechanism of orographic influence on asymmetry development also observed
 130 numerically^{7,8}. Indirectly²⁸, climatic variations led to different sequences of aggradation and
 131 degradation events in sedimentary basins flanking the range and resulted in a base-level more
 132 elevated on the leeward side than on the windward one¹⁰, a phenomenon that may also have
 133 influenced topographic asymmetry development. Assuming a symmetric topography at the onset of
 134 orographic barrier development 3 Myr ago²⁷, the subsequent estimated rate of divide migration is
 135 $\sim 0.8\text{-}1.5 \text{ mm yr}^{-1}$, of the same order of magnitude as uplift rates.

136 In natural settings, the spacing of drainage basin outlets along mountain fronts is remarkably
 137 regular, regardless of their tectonic and climatic settings^{9,29}. With the exception of some Himalayan
 138 catchments⁹, most landscapes obey a single empirical scaling law, which relates outlet spacing to half
 139 the distance between the main divide and the range front^{9,29}. As studied here, the experimental
 140 landscapes follow a similar law (see Supplementary Figure). In the context of widening mountain
 141 belts, the preservation of the spacing ratio implies that processes such as river capture or drainage
 142 divide collapse decrease the number of outlets during the lengthening of drainage basins^{9,29}. The
 143 present study demonstrates that the reverse occurs during the shortening of drainage basins induced
 144 by divide migration, and the split of drainage networks described here represents the only existing
 145 mechanism that allows to increase the number of drainage basins at mountain fronts and to
 146 maintain their spacing ratio. Experiments illustrate how complex the elevation history of a spatial
 147 point of a landscape can be. Many issues must still be investigated to better understand the
 148 mechanism of drainage splitting, both in experiments and nature; the channel behaviour at the
 149 tributaries' junction in the context of reducing discharge is likely the most important. However, the
 150 identification of the splitting mechanism provides the first opportunity to investigate drainage divide
 151 migration in active orogens through the coeval dynamics of the associated drainage networks.

152

153 METHODS

154 Experiments were performed in the Modelling Laboratory at Geosciences Rennes/University
 155 of Rennes1. I used a paste of pure silica grains (mean grain size of 20 μm) mixed with water. The
 156 water content was chosen such that the paste has a vertical angle of rest and water infiltration was
 157 negligible. The paste was introduced into a box with a vertically adjustable base, whose movements
 158 were driven by a screw and a computer-controlled stepping motor. The internal area of the box was
 159 60 X 40 cm and 50 cm deep. During an experimental run, the base of the box was raised at a constant
 160 rate and pushed the paste outside the top of the box at a rate defined as the uplift rate. Precipitation
 161 was generated by a system of four sprinklers that delivered water droplets with diameter of $\sim 10 \mu\text{m}$,
 162 which was small enough to avoid any splash dispersion at the surface of the model. The precipitation
 163 rate at the surface of the model could be controlled by changing the water pressure and the
 164 configuration of the sprinklers. Precipitation was measured by collecting water in 20 pans at the
 165 location of the model before and after each experimental run. The coefficient of variation (standard
 166 deviation/mean) of rainfall rates for measurement intervals of 10 minutes is less than 5 % for the

167 experiment performed here. The surface of the model was eroded by running water at its surface
 168 and grain detachment and transport occurred mainly by shear detachment through surface runoff.
 169 The topography was measured by using a commercial stereogrammetric camera system, which has a
 170 precision of ~20 µm. The raw data were gridded to produce DEMs with a pixel size of 0.5 mm.

171 Inherently to all laboratory modellings of landscape dynamics (at University of Rennes 1: see
 172 refs. 16, 17, 21 and at University of Minnesota: see ref. 14 and 15), experiments such as those
 173 developed here are oversimplifications of natural systems. Oversimplification is imposed by the
 174 difficulty to model some particular processes (vegetation dynamics, weathering processes and
 175 chemical erosion, atmospheric processes, etc.) but it is also a choice that is motivated by the
 176 necessity to understand the influence of each forcing parameter before investigating more complex
 177 systems. More importantly, experiments cannot be scaled to nature because of the impossibility to
 178 downscale natural conditions to the laboratory (for examples, see refs. 15, 17, 21). Because of these
 179 scale distortions, modelling of landscape dynamics is only experimental and not analog¹⁵⁻¹⁷. However,
 180 there is a consensus about the qualitative relevance of these models¹⁵⁻¹⁷, which permits a much more
 181 dynamic view of landscape evolution than the usual numerical models (see ref. 15).

182

183 References

- 184 1. Beaumont, C., Fullsack, P. & Hamilton, J. Erosional control of active compressional orogens.
 185 In *Thrust Tectonics* (ed McClay, K. R.) 1-18 (New York: Chapman Hall, 1992)
- 186 2. Hoffman, P. F. & Grotzinger, J. P. Orographic precipitation, erosional unloading, and tectonic
 187 style. *Geology* **21**, 195-198 (1993).
- 188 3. Willett, S. D. Orogeny and orography: The effects of erosion on the structure of mountain
 189 belts. *J. Geophys. Res* **104**, 28957-28981 (1999).
- 190 4. Montgomery, D. R., Balco G. & Willett, S. D. Climate, tectonics, and the morphology of the
 191 Andes. *Geology* **29**, 579-582 (2001).
- 192 5. Whipple, K. X. The influence of climate on the tectonic evolution of mountain belts. *Nature*
 193 *Geosci.* **2**, 97-104 (2009).
- 194 6. Willett, S. D., Slingerland, R. & Hovius, N. Uplift, shortening, and steady-state in active
 195 mountain belts. *Am. J. Sci.* **301**, 455-485 (2001).
- 196 7. Roe, G. H., Montgomery, D. R. & Hallet, B. Orographic precipitation and the relief of
 197 mountain ranges. *J. Geophys. Res.* **108** (2003) (doi:10.1029/2001JB001521).
- 198 8. Anders, A. M., Roe, G. H., Montgomery, D. R. & Hallet, B. Influence of precipitation phase on
 199 the form of mountain ranges. *Geology* **36**, 479-482 (2008).
- 200 9. Hovius, N. Regular spacing of drainage outlets from linear mountain belts. *Basin Res.* **8**, 29-44
 201 (1996).
- 202 10. Sobel, E. R. & Strecker, M. R. Uplift, exhumation and precipitation: Tectonic and climatic
 203 control of late Cenozoic landscape evolution in the northern Sierras Pampeanas, Argentina.
 204 *Basin Res.* **15**, 431-451 (2003).
- 205 11. Reiners, P. W., Ehlers, T. A., Mitchell, S. G. & Montgomery, D. R. Coupled spatial variations in
 206 precipitation and long-term erosion rates across the Washington Cascades. *Nature* **426**, 645-
 207 647 (2003).

- 208 12. Craw, D., Nelson, E. & Koons, P. O. Structure and topographic evolution of the Main Divide in
 209 the Landsborough-Hopkins area of the Southern Alps, New Zealand. *New Zealand J. Geol.*
 210 *Geophys.* **46**, 553-562 (2003).
- 211 13. Kuhlemann, J., Frisch, W., Dunkl, I., Székely, D. & Spiegel C. Miocene shifts of the drainage
 212 divide in the Alps and their foreland basin. *Z. Geomorph. N. F.* **45**, 239-265 (2001).
- 213 14. Hasbargen, L. E. & Paola, C. Landscape instability in an experimental drainage basin. *Geology*
 214 **28**, 1067-1070 (2000).
- 215 15. Hasbargen, L. E. Some Characteristics of Drainage Basin Realignment. *Eos Trans. AGU*, 87(36),
 216 *Jt. Assem. Suppl.*, Abstract H53F-04 (2006).
- 217 16. Bonnet, S. & Crave, A. Landscape response to climate change: Insights from experimental
 218 modeling and implications for tectonic versus climatic uplift of topography. *Geology* **31**, 123-
 219 126 (2003).
- 220 17. Lague, D., Crave, A. & Davy, P. Laboratory experiments simulating the geomorphic response
 221 to tectonic uplift. *J. Geophys. Res.* **108** (2003) (doi:10.1029/2002JB001893).
- 222 18. Whipple, K. X. & Tucker, G. E. Dynamics of the stream-power river incision model:
 223 Implications for height limits of mountain ranges, landscape response timescales, and
 224 research needs. *J. Geophys. Res.* **104**, 17661-17674 (1999).
- 225 19. Whipple, K. X. Fluvial landscape response time: How plausible is steady-state denudation?
 226 *Am. J. Sci.* **301**, 313-325 (2001).
- 227 20. Leopold, L. B. & Maddock Jr, T. The hydraulic geometry of stream channels and some
 228 physiographic implications. *U. S. Geol Surv. Prof. Pap.* **252** (1953).
- 229 21. Turowski, J. M., Lague, D., Crave, A. & Davy, P. Experimental channel response to tectonic
 230 uplift. *J. Geophys. Res.* **111** (2006) (doi:10.1029/2005JF000306).
- 231 22. Wobus, C. W., Tucker, G. E. & Anderson, R. S. Self-formed bedrock channels. *Geophys. Res.*
 232 *Lett.* **33** (2006) (doi:10.1029/2006GL027182).
- 233 23. Whittaker, A. C., Cowie, P. C., Attal, M., Tucker, G. E. & Roberts, G. P. Bedrock channel
 234 adjustment to tectonic forcing: Implications for predicting river incision rates. *Geology* **35**,
 235 103-106 (2007).
- 236 24. Strecker, M. R., Cervený, P., Bloom, A. L. & Malizia, D. late Cenozoic tectonism and landscape
 237 development in the foreland of the Andes: Northern Sierras Pampeanas (26°S-28°S),
 238 Argentina. *Tectonics* **8**, 517-534 (1989).
- 239 25. Strecker, M. R., Alonso, R. N., Bookhagen, B., Carrapa, B., Hilley, G. E., Sobel, E. R. & Trauth,
 240 M. H. Tectonics and climate of the Southern Central Andes. *Ann. Rev. Earth Planet. Sci.* **35**,
 241 747-787 (2007).
- 242 26. Bookhagen, B. & Strecker, M. R. Orographic barriers, high-resolution TRMM rainfall, and
 243 relief variations along the eastern Andes. *Geophys. Res. Lett.* **35** (2008)
 244 (doi:1029/2007GL032011).
- 245 27. Kleinert, K. & Strecker, M. R. Climate change in response to orographic barrier uplift: Paleosol
 246 and stable isotope evidence from the late Neogene Santa Maria basin, northwestern
 247 Argentina. *Geol. Soc. Am. Bull.* **113**, 728-742 (2001).
- 248 28. Sobel, E. R., Hilley, G. E. & Strecker, M. R. Formation of internally drained contractional basins
 249 by aridity-limited bedrock incision. *J. Geophys. Res.* **108** (2003) (doi:10.1029/2002JB001883).
- 250 29. Talling, P. J., Stewart, M. D., Stark, C. P., Gupta, S. & Vincent, S. J. Regular spacing of drainage
 251 outlets from linear faults blocks. *Basin Res.* **9**, 275-302 (1997).

252 30. Moyano, M. S. Análisis regional del emplazamiento, sedimentación y evolución sintectónica
 253 de los abanicos aluviales cuaternarios de las Sierras Pampeanas Nordoccidentales. Catamarca
 254 y Tucumán. Unpublished PhD thesis, Facultad de Ciencias Naturales e IML - Universidad
 255 Nacional de Tucumán, 209 p. (2009).

256

257

258 Correspondence and requests for materials should be addressed to S.B.

259

260 Acknowledgements

261 I would like to thank J.-J. Kermarrec for his technical assistance with the experiments and C.
 262 Andermann and M. Gaboriau for their friendly help during the experimental runs. This work
 263 benefited from discussions with B. Bookhagen, P.R. Cobbold, I. Coutand, A. Crave, P. Davy, D. Gapais,
 264 D. Lague and S. Moyano. Special thanks to P. Davy for providing and constantly improving the
 265 GridVisual software. This work was funded by the Institut National des Sciences de l'Univers (INSU-
 266 CNRS) through the "Reliefs de la Terre" research programme.

267

268

269 Figure captions

270 **Figure 1 Laboratory modelling of landscape dynamics under uniform uplift of the eroded material**
 271 **and lateral precipitation gradient.** The uplift rate is 12 mm h^{-1} . **a**, Evolution of topographic profiles.
 272 Each line is the mean elevation along a 20-cm-wide transverse swath calculated from DEMs. The
 273 patterns of rainfall forcing are also shown. Note the superimposition of the topographic profiles at
 274 the end of the first step, which implies a steady-state between uplift and erosion^{16,17}. **b**, Evolution of
 275 mean and maximum (drainage divide) elevations of the model. Error bars give the standard deviation
 276 of the mean. The solid line indicates the amount of applied uplift, i.e. elevation of the model if no
 277 erosion occurred. The line is only interrupted upward for graphical convenience; uplift forcing was
 278 applied during the entire experiment at a constant rate. Note that the constancy of mean and
 279 maximum elevations during the first evolution step implies a steady-state between uplift and
 280 erosion^{16,17} and the absence of a steady-state from the application of the rainfall gradient. **c**,
 281 Evolution of the normalized divide position⁶, highlighting the asymmetry development from the
 282 application of the rainfall gradient. **d**, Photographs of three stages of landscape evolution, taken at
 283 steady-state (600') and during the subsequent divide migration (940 and 1300'). The model width on
 284 the view is 400 mm.

285

286 **Figure 2 Landscape response to main drainage divide (MDD) migration.** The images are successive
 287 shaded surface views of the driest side of the model DEMs (views are $\sim 200 \times 300 \text{ mm}$) with
 288 superposition of drainage networks as extracted from DEMs using a steepest-slope flow routine. The
 289 width of individual channels on the images only depends on the pixel size of the DEMs (0.5 mm) and
 290 does not reflect the width dependency with discharge or slope. The images illustrate the migration of
 291 the MDD, the induced shortening of the drainage basins and the split of their drainage network. The
 292 splitting mechanism induced the abandonment of former parts of the landscape where tributaries

293 were initially connected (open arrows) and their subsequent uplift, leading to the development of
 294 new hillcrests (solid arrows). This mechanism consequently leads to the individuation of two
 295 drainage basins from a single former one.

296

297 **Figure 3 Detailed geomorphic evolution of a drainage basin.** **a**, Photographs taken from the
 298 driest side of the experimental landscape showing the location of the studied drainage basin (orange
 299 arrow) and of some selected points of the landscape whose elevation history is detailed. **b**, Time-
 300 evolution of mean runoff within the selected drainage basin, water flux at outlet and basin size. **c**,
 301 Time-evolution of the longitudinal profile of the main trunk channel. The stack of longitudinal profiles
 302 until 600 minutes corresponds to the steady-state between erosion and uplift during the first phase
 303 of uniform rainfall. Note the progressive shortening and steepening of the channel once the rainfall
 304 gradient is applied and the existence of a temporary steady-state before splitting occurred. **d**,
 305 Detailed elevation history of three selected points of the landscape. Point A is located in a channel
 306 and it remains in the channel during the entire experiment. After the application of the rainfall
 307 gradient, its elevation first increases but rapidly stabilizes during the temporary steady-state; it is
 308 finally uplifted after splitting occurred. Point B is located on a permanent hillcrest that separates two
 309 main drainage basins. It is continuously uplifted after the application of the rainfall gradient. The
 310 evolution of point C is a combination of histories of points A and B. It corresponds to a channel with a
 311 similar evolution than A until splitting occurred. It is then uplifted and ends on a hillcrest that divides
 312 up a former single drainage basin into two individual ones. Dotted lines show the trend of applied
 313 uplift (“rock uplift”) and therefore indicate the elevation of points that are passively uplifted, i.e.
 314 where no erosion occurred.

315

316 **Figure 4 Model of drainage basin response to drainage divide migration** (see text for comments).
 317 Blue colours show active streams, whereas orange colours show hypothetical floodplain deposits.
 318 Note that some of these deposits can be passively uplifted and observed on the hillcrest separating
 319 two newly-formed drainage basins. These deposits would be classically interpreted as resulting from
 320 relief inversion or river capture.

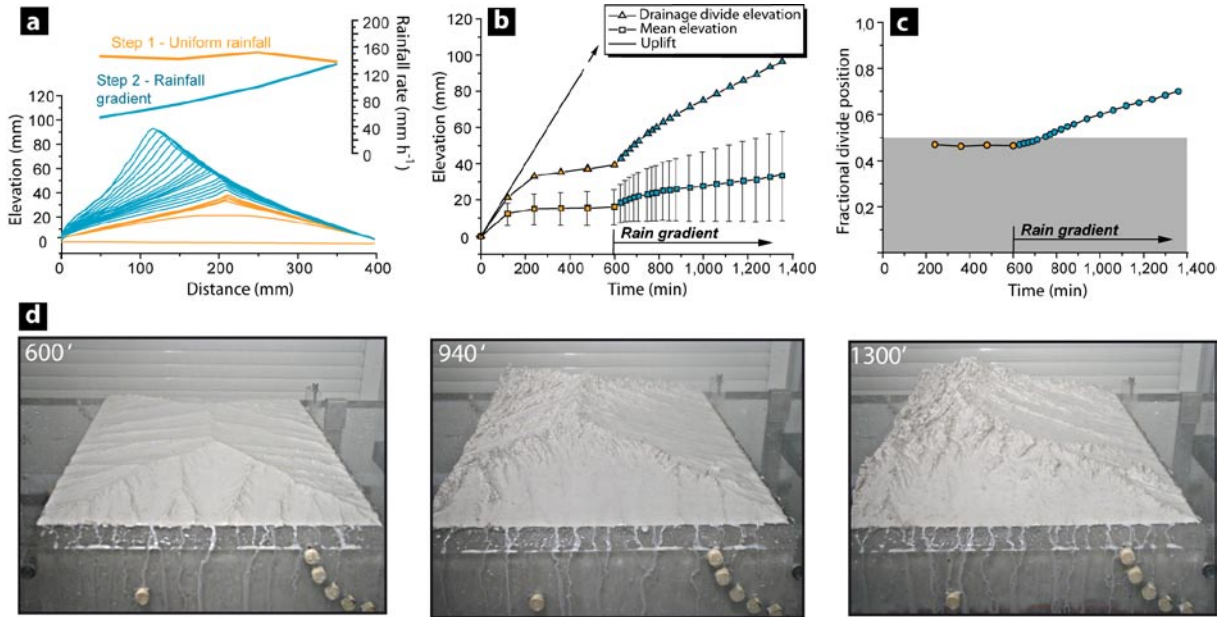
321

322 **Figure 5 Topography and drainage networks of the Sierra Aconquija, northwestern Argentina.** **a**,
 323 Map showing the topography of the Sierra Aconquija, major tectonic elements and mean annual
 324 precipitation (dotted blue lines, in mm yr⁻¹; after ref. 10). **b**, Perspective view highlighting the
 325 topographic asymmetry of the range. **c**, Images showing examples of drainage networks located on
 326 the driest side of the Sierra Aconquija where different stages of drainage splitting likely are
 327 represented, following the model shown in Fig. 4 (images from OpenAerialMap.org, except 1&2:
 328 GoogleEarth). Examples 1 and 2 are cases where two tributary streams do not connect at valleys’
 329 junction, but flow separately within a single valley floor (open arrows). The same configuration is
 330 observed in example 3, except that the two parallel-flowing streams are separated by elevated fluvial
 331 deposits (solid arrow) whose mapping³⁰ shows that they constituted a single alluvial body that
 332 extended upstream along the two streams. Consequently, it likely represents an example where

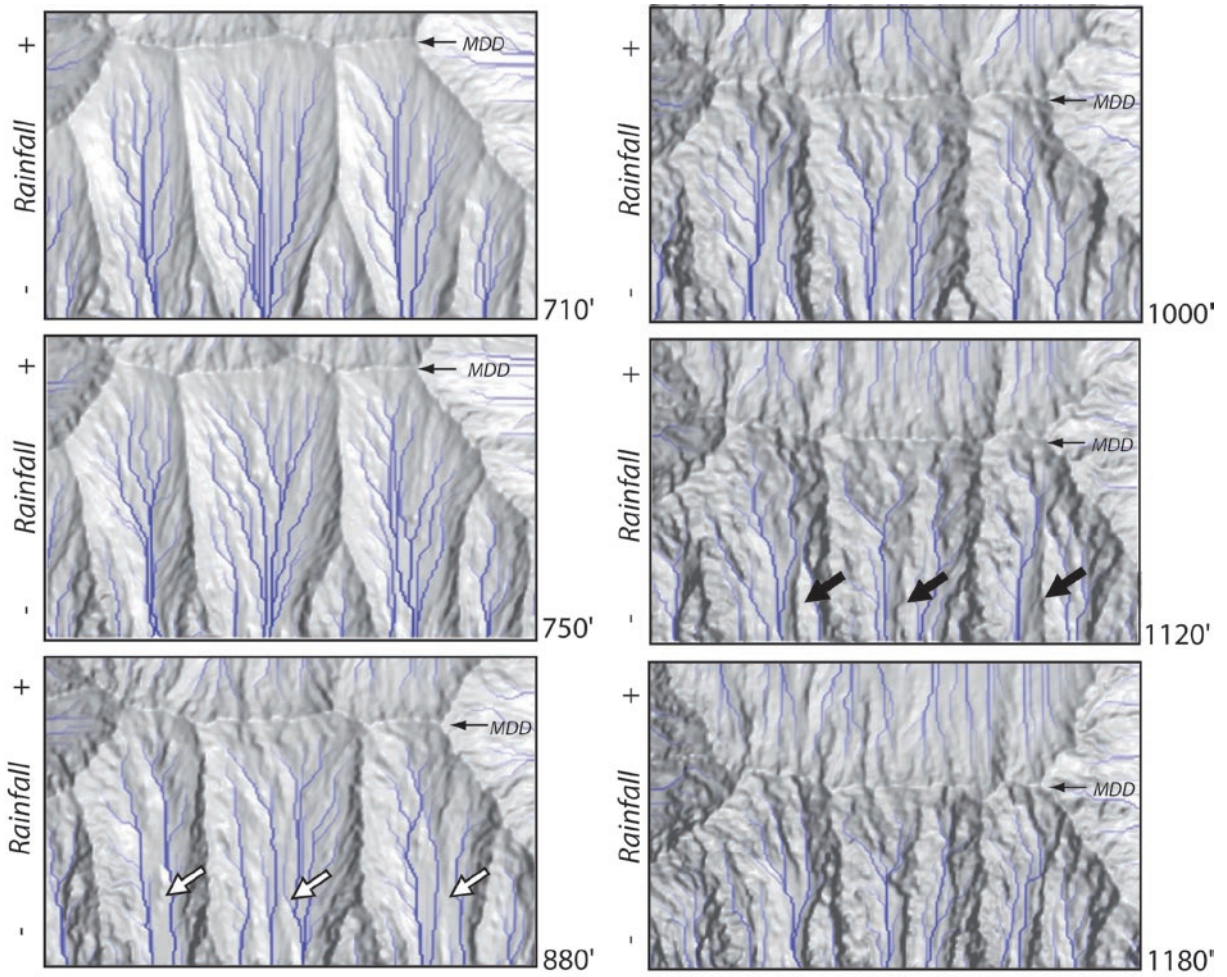
333 drainage splitting is associated to the nascent of a new hillcrest. Example 4 shows the case of a
334 hillcrest (solid arrow) separating two drainage basins whose outlets are very close and whose general
335 shapes suggest that they initially formed a single drainage basin. This assumption is reinforced by the
336 abrupt change in the flowpath direction of one river, suggesting a former connection between the
337 two drainage basins (white dotted line), and by the existence of a system of alluvial fans whose size
338 suggests feeding by a basin larger than the two present ones. This last example would thus represent
339 the ultimate case of the splitting mechanism.

340

341 **Supplementary Figure. Spacing of drainage basin outlets of experimental landscapes plotted**
342 **against drainage basin lengths.** The linear relationship shown here is similar to the trend observed in
343 natural landscapes⁹. The linear fit defines a spacing ratio (ratio between the spacing and the length⁹)
344 of 2.22, whereas the values range between 1.91 and 2.23 in natural landscapes⁹.

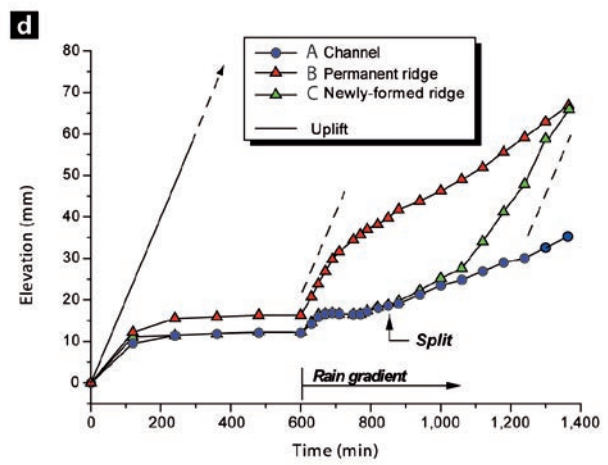
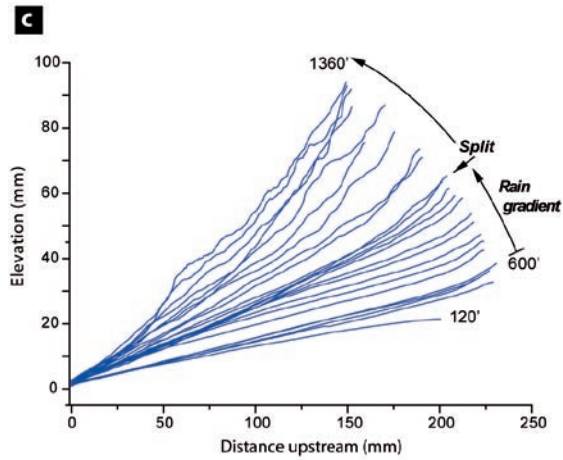
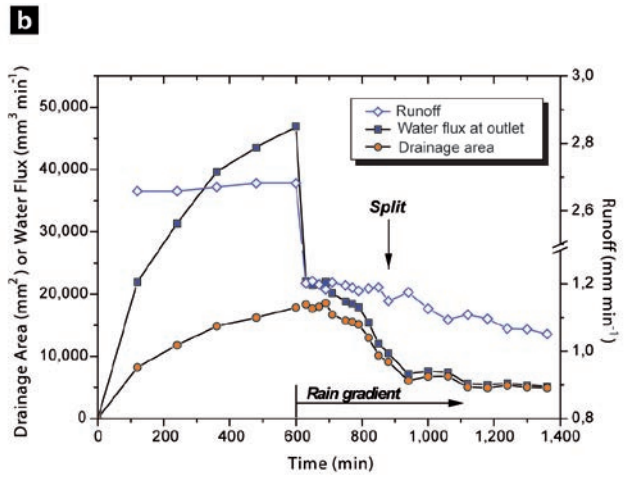


345 NGS-2009-06-00693
BONNET Figure 1



NGS-2009-06-00693
BONNET Figure 2

346

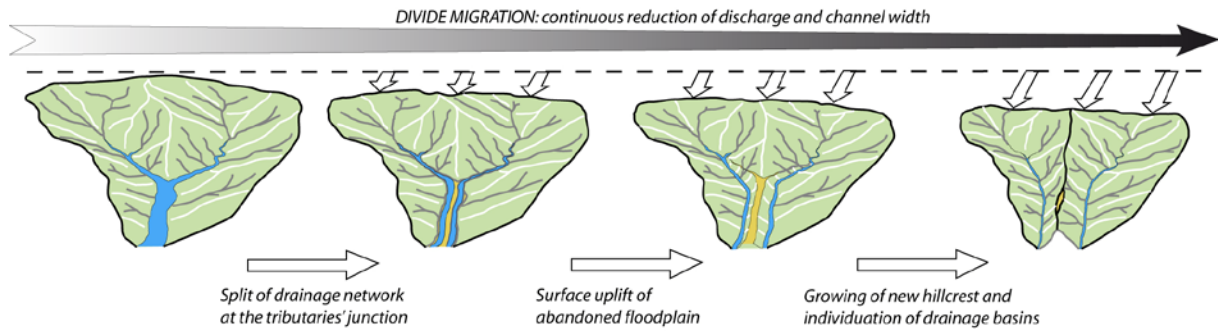


NGS-2009-06-00693
BONNET Figure 3

347

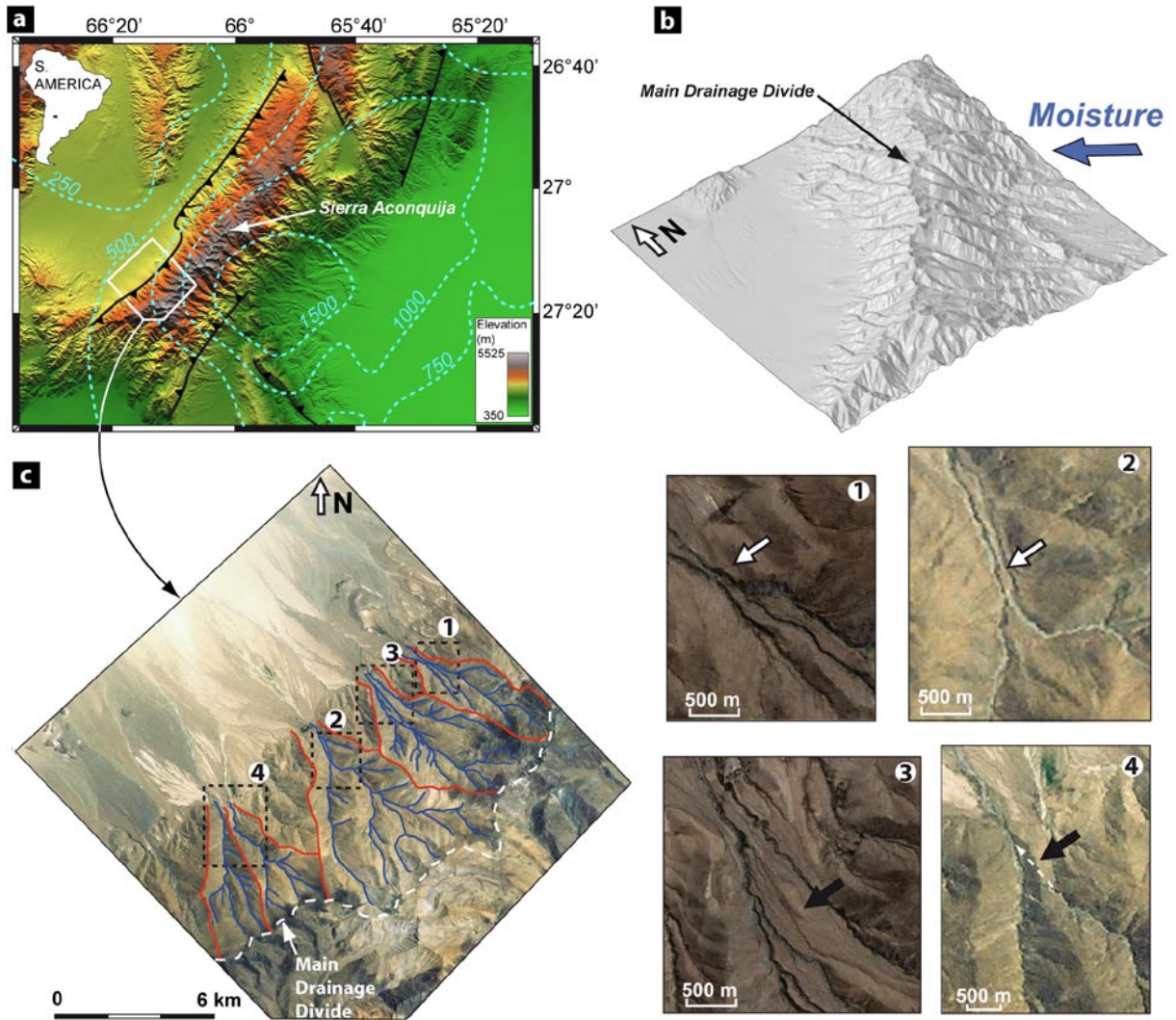
348

349



NGS-2009-06-00693
BONNET Figure 4

350



NGS-2009-06-00693
BONNET Figure 5

351